Photochromic point-diffraction inteferometer

Martino Quintavalla [a,b], Giorgio Pariani [a], Giuseppe Crimi [a], Chiara Bertarelli [b], Andrea Bianco [a,*]

[a] INAF-Osservatorio Astronomico di Brera, via Bianchi 46, 23807 Merate, Italy
[b] Politecnico di Milano, Dipartimento di Chimica, Materiali ed Ingegneria Chimica, Piazza L. da Vinci 32, 20133 Milano, Italy

Article history:
Received 8 August 2013
Received in revised form
10 December 2013
Accepted 10 December 2013
Available online 14 January 2014

1. Introduction

The reversible light-induced change of color of a chemical species, known as photochromism [1], has been exploited for more than 40 years to produce photochromatic lenses, where the optical density is the result of the equilibrium between coloration and fading induced by sunlight absorption and ambient temperature [2]. Accordingly, photochromic layers are tuneable filter, as the color variation turns into a light-induced change in their transmittance in a specific spectral region. This color variation is accompanied by the modification of many physical–chemical properties of the materials [3] which leads to the development of smart light controlled devices, such as rewritable optical memories [4], tuneable masks, amplitude holograms, and volume gratings [3]. Recently, we have used photochromic materials to develop adaptable tools for testing the quality of optical elements, specifically rewritable amplitude Computer Generated Holograms (CGHs) based on the strong modulation of transparency in the visible region of photochromic polyurethane layers [5]. Going forward with this idea, we herein demonstrate a point-diffraction interferometer (PDI) based on thermally irreversible photochromic materials. The PDI, which is a common path interferometer invented by Linnik in 1933 and further developed by Smartt in the 70s [6], has found a widespread use in the optics industry due to its ease of implementation and operation, stability to vibrations and low sensitivity to air turbulence in comparison to other interferometers [7–10]. Such features make the PDI the ideal interferometer for an in situ metrology of even very large optics in hard environments. Moreover, the PDI being a self-referencing interferometer, it does not require an expensive reference surface. This is not the case of the Fizeau interferometer. Basically, the PDI consists of a semi-transparent substrate with a pinhole or an opaque dot, on which the converging test beam is focused (Fig. 1).

If the size of the pinhole is of the order of half the size of the Airy disc, part of the incident light is diffracted and generates a nearly perfect spherical wavefront that acts as the reference beam. The portion of light passing through the semi-transparent surrounding area (which contains the information about the optics surface figure) is attenuated and makes interference with the reference beam. The analysis of the resulting interferogram provides the characterization of the optics under test and its aberrations. The size of the pinhole and the transparency of the outer region are the two key parameters governing the relative intensities of the reference and the test beams and, accordingly, the quality of the interferogram, expressed in terms of fringe visibility. The visibility V is defined as follows [11]:

$$V = \frac{I_{max} - I_{min}}{I_{max} + I_{min}} \quad (1)$$

where I_{max} and I_{min} are the intensities of the bright and dark areas, respectively. In particular, the size of the pinhole affects the angular aperture, intensity, and accuracy of the reference beam [8]. Indeed, the larger the pinhole, the higher the light intensity, but the lower the precision of the wavefront, which is more affected by shape errors of the pinhole [10,12,13]. Usually, the pinhole diameter is fixed and is determined by the production

* Corresponding author. Tel.: +39 0395971060; fax: +39 0395971001.
E-mail address: andrea.bianco@brera.inaf.it (A. Bianco).

method of the PDI itself (typically photolithography, etching or random-dot filtering [9,14,15]). This means that different PDIs are required to test optics with different focal ratios. The semi transparency of the regions outside the pinhole is also fixed so the fringe visibility cannot be optimized. Some attempts toward the improvement of visibility have been made, e.g., by using polarization-sensitive filtering where a pinhole is etched into a polarized plate whose rotation determines the intensity of the test beam [14,15].

The possibility to easily tune the transparency of photochromic materials is a powerful methodology to develop versatile PDIs. The opaque state of the photochromic layer is induced by UV light, then transparent pinholes of different sizes can be optically written by locally converting the layer using a visible light source. In this way the PDI can be adapted to test optics with different features. This conversion phenomenon can also be exploited to bleach, in a controlled fashion, the opaque outer region to increase its transparency and balance the intensities of the two interfering beams. This turns into a maximization of the fringe visibility. Moreover, the reversibility of the photochromic reaction makes the system completely rewritable, thus further enhancing the versatility of photochromic PDIs.

2. Methods and materials

According to the description of the PDI, the most important parameter to consider is the contrast of the photochromic layer at the test wavelength, *CT*, which is defined as the ratio between the transmittance of layer in the colored and uncolored states:

$$CT = \frac{T_{\text{uncolored}}}{T_{\text{colored}}} \cong \frac{1}{T_{\text{colored}}} = 10^{A_{\text{colored}}} = 10^{\varepsilon CZ} \tag{2}$$

where ε is the absorption coefficient, C the concentration of the photochromic moiety and Z the film thickness. Since the uncolored form is transparent in the visible region, it is possible to assume

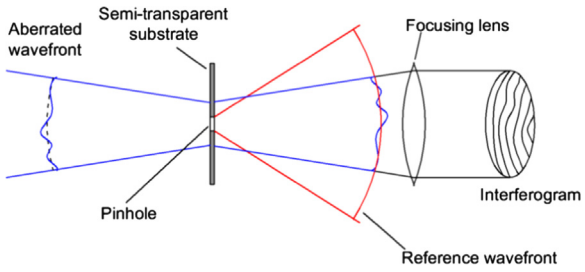

Fig. 1. Functioning scheme of a Point Diffraction Interferometer (PDI).

$T_{\text{uncolored}} = 1$. Therefore, the contrast is only a function of the transmittance of the colored state. As T_{colored} determines the maximum opacity of the semi-transparent area the larger this parameter the wider the possibility of tuning the fringe visibility. According to the Lambert–Beer's law (Eq. (2)), high contrast means thick films (Z) with a large content of photochromic dye (C), and a high absorption coefficient (ε) in the colored state. From the various strategies available to produce a photochromic substrate fulfilling these requirements, we have focused our attention on the synthesis of polymers with photochromic units in the main chain. Such polymers allow us to maximize the sensitivity of the layer [16].

To produce the photochromic substrate we referred to a diarylethene-based polyurethane coating we recently developed for optical applications; this coating shows a notable contrast and good optical quality (Fig. 2) [17]. The formulation enables the optical properties of the photochromic layer to be customized by varying the chemical structure and the amount of the photochromic monomer. The solution containing the reactants is cast on functionalized borosilicate glass substrates by spin or control coating, and the complete polymerization is achieved after a heat treatment of 12 h at 120 °C. The thickness of the resulting layers, measured by spectral reflectance (Filmetrics F20EXR), depends on the casting parameters and can be varied from 1 to 10 μm. Photochromic films show uniform thickness, high homogeneity, and contrasts up to 10^4 at 633 nm. Ultra violet (UV)-vis absorption spectra of a layer with an active unit content of 30 wt% under different exposures to UV light (366 nm) are reported in Fig. 2.

Once the photochromic layer is converted to the opaque form with UV light, the pinholes are optically written with a custom-made apparatus consisting of a He–Ne laser source (633 nm) properly attenuated by a polarizing filter and focused onto the photochromic substrate, providing a minimum spot size of 2 μm. The substrate is mounted on a rotating and translating stage to write both pinholes and auxiliary alignment markers. Since the photochromic conversion is a non-linear process [18] (i.e. the conversion becomes faster as the light intensity increases), it is possible to write pinholes in a wide range of dimensions by keeping the spot size constant and varying the photon dose (namely, exposure time and light intensity) with a single laser pulse. Simulations of the photochromic conversion under a Gaussian beam exposure of constant size clearly show that the pinhole diameter increases while increasing the photon dose [19], as shown in Fig. 3(a). In Fig. 3(b), microscope images of pinholes experimentally obtained at the same conditions confirm this behavior. This feature is worth noting since it makes the writing procedure very simple and unaffected by any parameter other than the optical quality of the focusing lens. The pinholes diameter

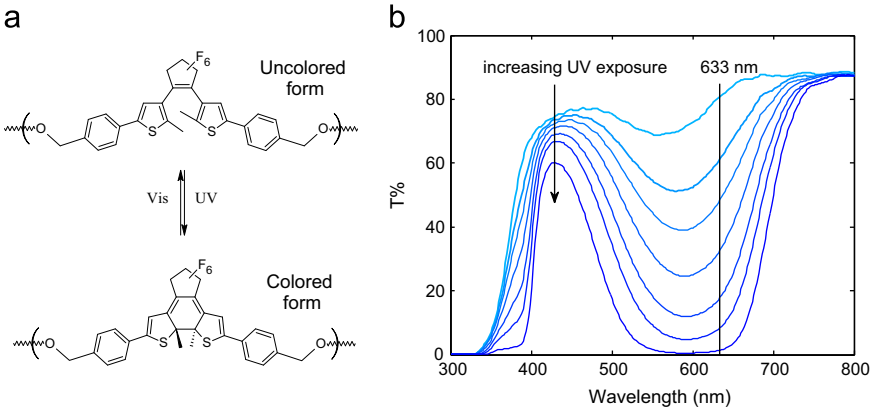

Fig. 2. (a) Photochromic reaction of the diarylethene unit in the polyurethane coating; and (b) UV–vis absorption spectra of a photochromic film with a content of photochromic units of 30 wt% (right).

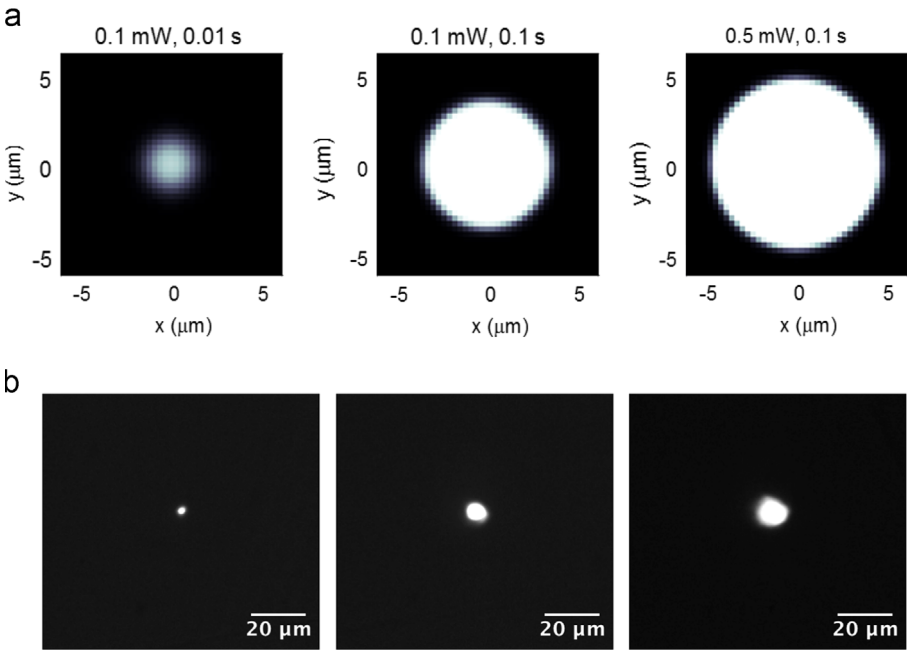

Fig. 3. (a) Images of the pinhole obtained from the simulation; and (b) optically written pinholes on a photochromic substrate varying the time and the light intensity.

Table 1
Circularity and diameters of the written pinholes and a comparison with the simulated diameters.

Pinhole power (mW)/time (s)	Circularity*	Diameter (μm)	Diameter (μm) from simulations
0.1/0.01	0.95	2.2	2.4
0.1/0.1	0.90	6.4	6.6
0.5/0.1	0.90	9.0	9.0

* The circularity is defined as: $4\pi A/P^2$, where A is the area of the pinole and P its perimeter.

varies from 2 to 10 μm, making the photochromic PDI suitable for testing optics with a wide range of focal (f) ratios (approximately from $f/2$ to $f/8$ considering the pinhole size as the half of the Airy disc at 633 nm). Due to the quality of the focusing lens and to the non-linearity of the photochromic conversion, a slight decrease of pinhole circularity is observed for increasing pinhole sizes (Table 1).

The optical test setup is depicted in Fig. 4. The photochromic film with the written pinhole is mounted at the center of curvature of a spherical mirror. The setup is equipped with an additional light source (a 650 nm laser diode, 50 mW) that can be used to bleach the photochromic film in order to tune the semi transparency of the outer region and maximize the fringe visibility.

3. Results and discussion

The first tests were carried out on a low quality spherical mirror ($f/2.65$ mirror of 150 mm in diameter) in order to measure the fringe visibility as a function of the transparency of the photochromic layer. The procedure is as follows: the substrate with a 2 μm diameter pinhole was mounted in the interferometric setup and positioned in such a way that a few fringes were visible on the interferogram; a single image was recorded with the CCD camera (typical exposure time of 100 ms) and the fringe visibility was measured; then the bleaching laser was turned on and the photochromic film was bleached for 5 s. A new frame was obtained and the visibility was measured again. This procedure

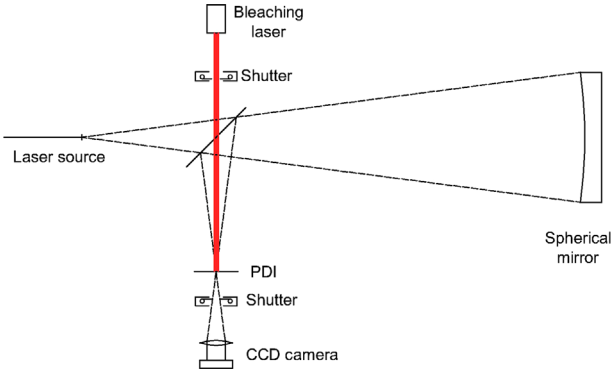

Fig. 4. Schematic of the interferometric setup for the test of spherical mirrors with the photochromic PDI.

was repeated until the fringe visibility became very low. Image analysis provided the trend of the fringe visibility as function of the bleaching time, as reported in Fig. 5(a).

During the bleaching, the fringe visibility initially increases reaching a maximum, then it decreases, as expected. At the beginning, the intensity of the reference beam is larger than the test beam (photochromic layer too opaque) while at the end it is lower (photochromic layer too transparent).

Once proved the possibility to optimize the fringe visibility, different tests were carried out in order to understand the reliability of the photochromic PDI and its limits in terms of measurement accuracy. It is worth mentioning that optics with $\lambda/20$ (30 nm) Root Mean Square (RMS) figure errors are usually considered of high quality for optical applications. In order to verify the performances of the photochromic PDI in the most demanding cases, we tested a number of mirrors of surface quality in the range of $\lambda/20$ RMS or better. In particular, mirrors with different focal ratios were measured and the results are reported on (i) a self-referencing test to discriminate the errors originated by the interferometric setup and by pinhole shape errors, (ii) the stability and repeatability test of the measurements, (iii) the comparison between the results obtained with the PDI and with a standard Fizeau interferometer (Zygo GPI XP) and (iv) a very high

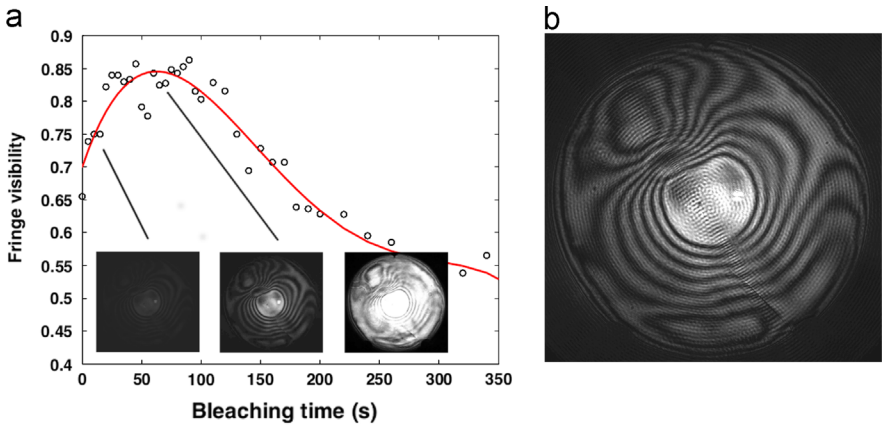

Fig. 5. Photochromic PDI: (a) fringe visibility of the *f*/2.65 mirror as function of the bleaching time; (b) example of interferogram recorded under the conditions of maximum fringe visibility.

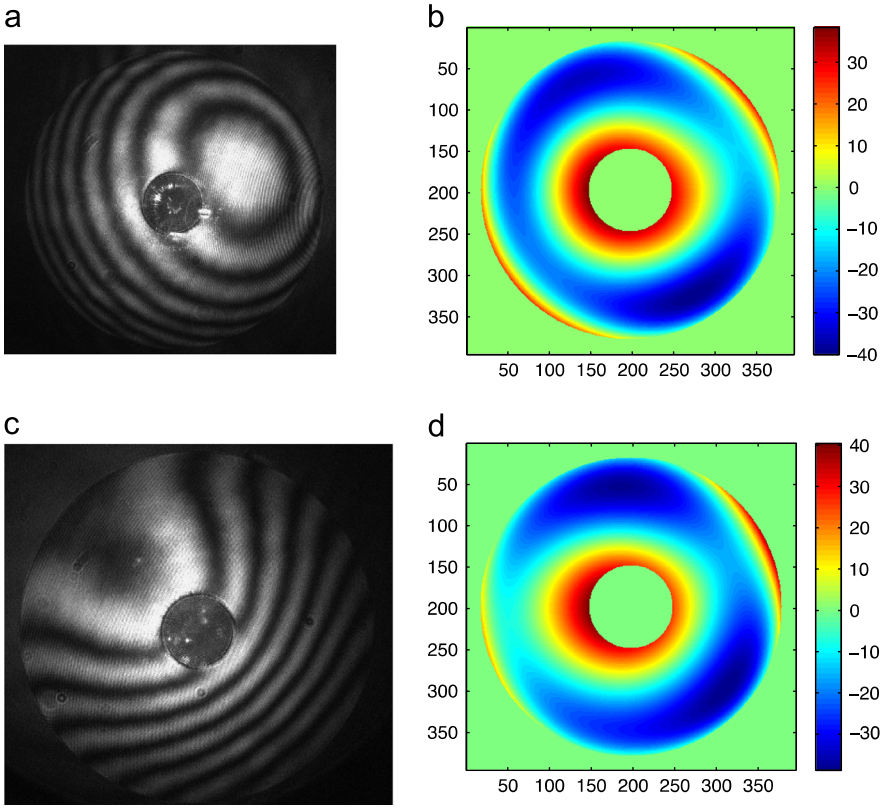

Fig. 6. Two examples of interferograms and OPDs for the *f*/2 spherical mirror with a central hole recorded with the photochromic PDI for two different orientations: (a) interferogram at 0°; (b) OPD at 0°; (c) interferogram at 180°; and (d) OPD at 180°. OPD values are in nanometers.

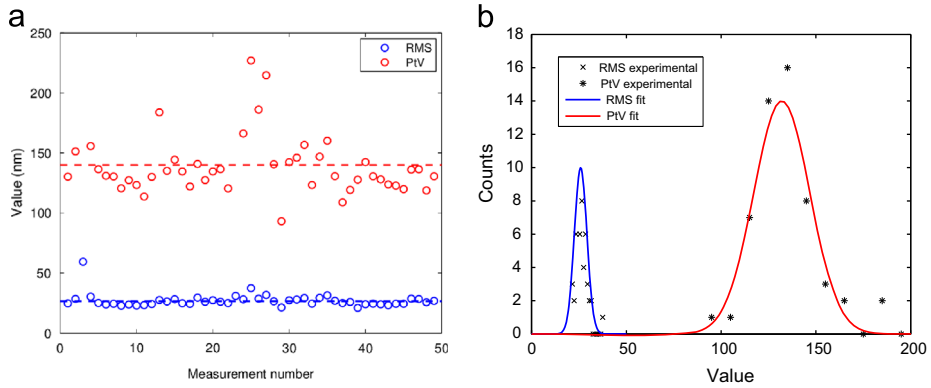

Fig. 7. Measurements of the *f*/2 spherical mirror: (a) RMS and PtV values for the 50 measurements; and (b) the normal distribution fitting for the same measurements.

quality certified mirror to understand the best performances of the photochromic device.

For the self-referencing test, a spherical $f/2$ mirror with a diameter of 150 mm was measured at 0° and 180° of rotation along its axis. A photochromic PDI with a 2.5 μm diameter pinhole was mounted in the optical setup and the fringe visibility was properly optimized. Fifteen interferograms were recorded and analyzed with a fringe interpolating software [20] that returned the Optical Path Difference (OPD) map of the surface as a sum of the first 25 Zernike polynomials. Interferograms and fitted OPDs of the measurements at 0° and 180° are reported in Fig. 6.

The two interferograms differ from the number of tilt fringes that have been introduced. Nevertheless, OPDs are very similar: for the 0° orientation a RMS value of 27 nm and a Peak to Valley (PtV) value of 128 nm have been measured; for the 180° orientation, RMS is 22 nm and PtV is 126 nm. These results show that the errors introduced by the PDI elements are small.

The repeatability test was performed on the same mirror. A set of 50 measurements were carried out, by realigning each time the pinhole and varying the number of the introduced tilt fringes. Therefore, they can be considered as 50 independent measurements. The results obtained from the analyses of the recorded interferograms in terms of RMS and PtV are reported in Fig. 7(a) together with their distribution (Fig. 7(b)).

RMS and PtV values are consistent and stable over the whole measurements. A PtV value of 132 nm with a standard deviation of 15 nm and an RMS value of 26 nm with a standard deviation of 3 nm are obtained. The standard deviations are one order of magnitude smaller than the averages, meaning that the measurements are consistent. As a general evidence, reliable results are achieved by averaging at least 10 measurements.

In a following test, PDI results were compared with those coming from the standard Fizeau interferometer. Fig. 8 shows the two OPDs and RMS and PtV values with their standard deviations of the $f/2$ mirror measured with the two interferometers are listed in Table 2.

As shown in the pictures, OPD shapes are very similar, and the RMS and PtV values are in good agreement. The standard deviation of the measurements is, in absolute, small for both the interferometers, but it is slightly larger for the PDI. This evidence is mainly ascribed to the absence of the phase shifting technique in the PDI with respect to the Fizeau interferometer which, in turn, requires a smaller number of measurements to yield comparable error levels. It is well-known that phase shifting is employed to decrease both absolute and statistical errors in interferometric measurements [21]. With a more complex setup, phase shifting may also be implemented in the PDI to reduce the statistical errors, as examples in the literature report [7,10,15].

Finally, a certified 6" $f/8$ $\lambda/8$ PtV and $\lambda/40$ RMS spherical mirror was tested in order to show the behavior of the PDI with a very high quality mirror, pushing its limit. This mirror has a very good optical quality and a very long focal length, providing an optical path of 2.4 m between the mirror and the PDI. A pinhole of about 7 μm was written and again the fringe visibility optimized. The results were obtained by averaging 50 different measurements. Fig. 9 reports the OPD of the mirror and the measured values for RMS and PtV and their standard deviations are listed in Table 3.

Values are in good agreement with the mirror specifications (confirming that the errors introduced both by the pinhole shape

Table 2
Comparison among the results obtained with PDI and the reference Fizeau interferometer.

	OPD (nm) RMS	Std. dev. (nm) RMS	OPD (nm) PtV	Std. dev. (nm) PtV
Fizeau interferometer	29	2	144	9
PDI	26	3	132	15

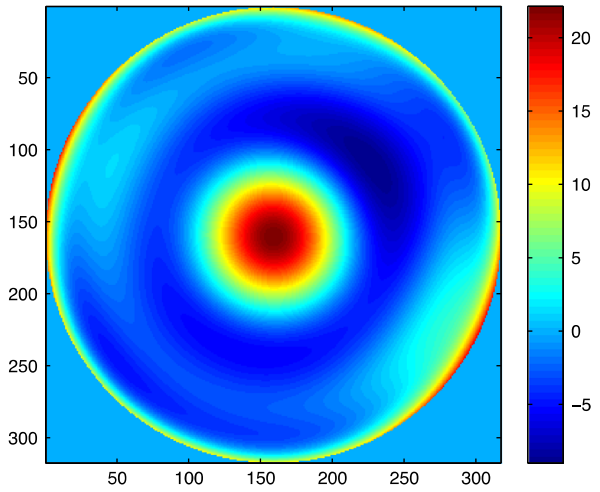

Fig. 9. OPD of the certified 6" $f/8$ $\lambda/8$ PtV and $\lambda/40$ RMS spherical mirror (values are in nanometers).

Table 3
RMS and PtV surface errors with their standard deviations for the certified 6" $f/8$ $\lambda/8$ PtV and $\lambda/40$ RMS spherical mirror.

RMS surf. error (nm)	8.5
RMS std. dev. (nm)	2
PtV surf. error (nm)	56
PtV std. dev. (nm)	17

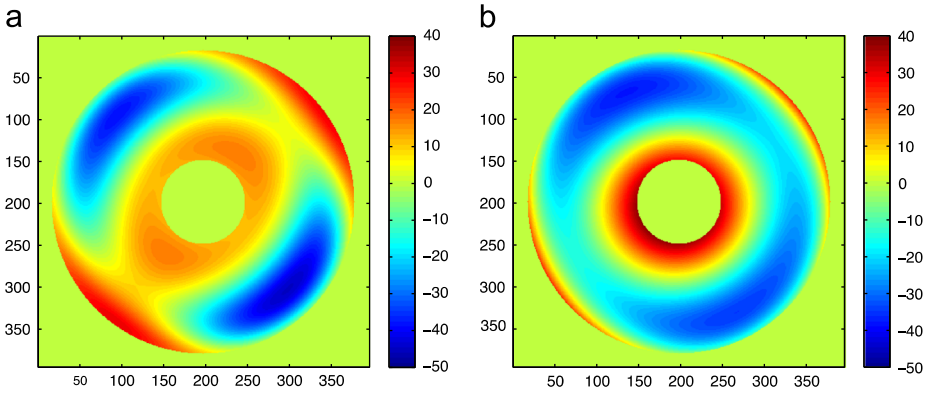

Fig. 8. OPDs of the $f/2$ spherical mirror: (a) from the Fizeau interferometer; and (b) from the PDI; all values are in nanometers.

and by air turbulence and vibrations are less than 10 nm RMS), which make the photochromic PDI competitive with the standard interferometric techniques.

4. Conclusion

We have demonstrated the good performance of a versatile Point-Diffraction Interferometer based on photochromic optical coatings. The photochromic PDI is rewritable and fully reconfigurable, by changing the pinhole size and the semi transparency of the outer region. The system is reliable in testing optical elements of high quality and on very different numerical apertures (from *f*/8 to *f*/2), showing good accuracy and repeatability.

There are some possibilities to further enhance the performances of the photochromic PDI, in particular: (i) increase the contrast of the photochromic substrate, thus allowing the use of smaller pinholes (better reference wavefront); (ii) improve the circularity of the pinholes; and (iii) perform an absolute calibration of the optical setup with a referenced method [22], in order to take into account the aberrations introduced by the optical components in the interferometric path (beam splitter and relay optics).

Acknowledgment

This work was partly supported by the Regione Lombardia through the MITO project and by the European Community (FP7-OPTICON).

References

[1] Bouas-Laurent H, Dürr H. Organic Photochromism. Pure Appl. Chem. 2001;73:639–65.
[2] Crano JC, Flood T, Knowles D, Kumar A, VanGemert B. Photochromic compounds: chemistry and application in ophthalmic lenses. Pure Appl. Chem. 1996;68:1395–8.
[3] Bianco A, Perissinotto S, Garbugli M, Lanzani G, Bertarelli C. Control of optical properties through photochromism: a promising approach to photonics. Laser Photonics Rev. 2011;5:711–36.
[4] Irie M. Diarylethenes for memories and switches. Chem. Rev. 2000;100:1685–716.
[5] Pariani G, Bertarelli C, Dassa G, Bianco A, Zerbi G. Photochromic polyurethanes for rewritable CGHs in optical testing. Opt. Express 2011;19:4536–41.
[6] Smartt RN, Steel WH. Theory and application of Point-Diffraction interferometers. Jpn. J. Appl. Phys. 1975;14:351–6.
[7] Millerd JE, Brock NJ, Hayes JB, Wyant JC. Instantaneous phase-shift point-diffraction interferometer. Proc. SPIE 2004;5531:264–72.
[8] Koliopoulos C, Kwon O, Shagam R, Wyant JC, Hayslett CR. Infrared point-diffraction interferometer. Opt. Lett. 1978;3:118–20.
[9] Furuhashi H, Shibata A, Uchida Y, Matsuda K, Grover CP. A point diffraction interferometer with random-dot filter. Opt. Commun. 2004;237:17–24.
[10] Mercer CR, Creath K. Liquid-crystal point-diffraction interferometer for wavefront measurements. Appl. Opt. 1996;35:1633–42.
[11] Born M, Wolf E. Principles of Optics. Oxford: Pergamon Press; 1980; 267.
[12] Anderson CS. Fringe visibility, irradiance, and accuracy in common path interferometers for visualization of phase disturbances. Appl. Opt. 1995;34:7474–85.
[13] Gao F, Jiang Z-D, Li B. Diffraction wavefront analysis of point diffraction interferometer for measurement of aspherical surface. Proc. SPIE 2010;7656:76565Y.
[14] Wang D, Yang Y, Chen C, Zhuo Y. Point diffraction interferometer with adjustable fringe contrast for testing spherical surfaces. Appl. Opt. 2011;50:2342–8.
[15] Neal RM, Wyant JC. Polarization phase-shifting point-diffraction interferometer. Appl. Opt. 2006;45:3463–76.
[16] Wigglesworth TJ, Myles AJ, Branda NR. High-content photochromic polymers based on dithienylethenes. Eur. J. Org. Chem. 2005:1233–8.
[17] Pariani G, Castagna R, Dassa G, Hermes S, Vailati C, Bianco A, et al. Diarylethene-based photochromic polyurethanes for multistate optical memories. J. Mater. Chem. 2011;21:13223–31.
[18] Pariani G, Bianco A, Castagna R, Bertarelli C. Kinetics of photochromic conversion at the solid state: quantum yield of dithienylethene-based films. J. Phys. Chem. A 2011;115:12184–93.
[19] Bianco A, Pariani G, Zanutta A, Castagna R, Bertarelli C. Photochromic materials for holography: issues and constraints. Proc. SPIE 2012;8281:828104.
[20] Fringe X.P. 2003. ⟨http://www.ceravolo.com/fringeXP.html⟩.
[21] Malacara D. Optical Shop Testing (Third Edition), New Jersey: A. John Wiley & Sons Inc.; 2007, pp. 547–552.
[22] Malacara D. Optical Shop Testing (Third Edition), New Jersey: A. John Wiley & Sons Inc.; 2007, pp. 72–73.